Interaction between droplets in a ternary microemulsion evaluated by the relative form factor method

Michihiro Nagao*
Cyclotron Facility, Indiana University, Bloomington, Indiana 47408-1398, USA
and NIST Center for Neutron Research, National Institute of Standards and Technology, Gaithersburg, Maryland 20899-8562, USA

Hideki Seto
Department of Physics, Graduate School of Science, Kyoto University, Kyoto 606-8502, Japan

Norifumi L. Yamada
Institute of Materials Structure Science, High Energy Accelerator Research Organization, Tsukuba 305-0801, Japan
(Received 14 November 2006; revised manuscript received 16 February 2007; published 6 June 2007)

This paper describes the concentration dependence of the interaction between water droplets coated by a surfactant monolayer using the contrast variation small-angle neutron scattering technique. In the first part, we explain the idea of how to extract a relatively model free structure factor from the scattering data, which is called the relative form factor method. In the second part, the experimental results for the shape of the droplets (form factor) are described. In the third part the relatively model free structure factor is shown, and finally the concentration dependence of the interaction potential between droplets is discussed. The result indicates the validity of the relative form factor method, and the importance of the estimation of the model free structure factor to discuss the nature of structure formation in microemulsion systems.

DOI: 10.1103/PhysRevE.75.061401 PACS number(s): 82.70.Uv, 68.05.Gh, 61.12.Ex

I. INTRODUCTION

Small-angle scattering techniques provide knowledge of the shape, structure, and interaction of objects in the nanometer scale. Especially, for understanding complex systems, such as membranes, biomolecular systems, etc., small-angle neutron scattering (SANS) is quite powerful because the scattering contrast of the components can be changed by selective deuteration of the hydrogen atoms. However, the data reduction procedure of SANS is usually difficult when the system is relatively concentrated, so that the effect of the structure factor is essential. Since the structure factor contains information about the interaction among scatterers, the extraction of the structure factor from the small-angle scattering data helps us to understand the nature of the structure formation of the systems.

So far, much effort has been made to estimate the form factor and the structure factor simultaneously in colloidal systems with very few assumptions. The generalized indirect Fourier transformation method developed by Glatter *et al.* [1,2] is one possible candidate. In this technique, the form factor of the system can be estimated as a direct space correlation function without any assumptions of the shape of the particle structure. However, the contribution from the structure factor is treated as an assumption of the model structure factor. Another candidate is the procedure by Arleth and Pedersen [3] by using a contrast variation SANS technique. They performed a simultaneous fitting to several scattering profiles with different contrasts taking the size polydispersity effect into account. They assumed a model structure factor for the polydisperse hard-sphere case, and evaluated the structure parameters relating to the shape of the object precisely. However, an assumption about the structure factor is still necessary, and the confirmed concentration region is limited.

Recently, a new SANS data reduction procedure was proposed by independent groups [4,5], which we call the relative form factor method. Using the contrast variation SANS technique, the scattering intensities for two different contrast conditions were measured. The ratio of these intensities can be the ratio of the form factors for each contrast condition, since the profile of the structure factor does not depend on the scattering contrast. Therefore, without any assumptions about the profile of the structure factor, the form factor can be evaluated. Once the form factor is known, the structure factor can be calculated from the scattering intensity. This method has first been applied to the spherical object [4–6] and then extended to the rod and the disk objects [7,8].

As a model spherical microemulsion system, we employed a system composed of AOT (dioctyl sulfossucinate sodium salt), water, and decane. This system has been intensively investigated by many researchers for some decades. The characteristic features of the AOT microemulsion are as follows: A single phase microemulsion being a water-in-oil droplet structure is stable in the large area of the ternary phase diagram at room temperature [9]. At a fixed molar ratio of water to AOT, W, the droplet size remains constant and the droplet density changes depending on the concentration of oil. The droplet density, ϕ, is determined as $\phi=(\phi_w+\phi_s)/(\phi_w+\phi_s+\phi_o)$, where ϕ_w, ϕ_s, and ϕ_o are the volume fractions of water, amphiphile, and oil, respectively. At the dilute droplet regimes, a phase decomposition from a single phase droplet into two phase coexistence of the droplet rich and poor domains associated with critical phenomena occurred with increasing temperature [9–14]. This is due to the increase of an attractive interaction between droplets with

*Electronic address: mnagao@indiana.edu

increasing temperature, and a cluster formation of droplets is considered to explain the experimental results [15]. At a semi-dilute to dense droplet regime ($\phi > 0.4$), a phase transition from droplet to lamellar structure occurred with increasing temperature [16–18]. The concentration dependence of the structures were investigated by some groups using small-angle x-ray scattering (SAXS) or SANS [19,20]. In their analyses, assumptions of the form factor and/or the structure factor were necessary to deduce information about the systems. This fact means that a model dependence of the small-angle scattering data analyses could not be avoided.

According to these experimental investigations, the AOT microemulsion system has been considered to be a rather simple system. However, unsolved issues are still remaining. In the phase diagram, a phase separation between one-phase and two-phase droplets is observed with elevating temperature in the low concentration region, while a phase transition from the one-phase droplet to the lamellar structure is observed above $\phi \approx 0.4$ [17]. This fact suggests that the dominant interaction between droplets for such phase transitions is different between the lower and the higher concentration regions.

It is also known that there is a percolation threshold in the droplet phase. The origin of the percolation is described by Chen *et al.* [16]. They claimed that a short-range attractive interaction between droplets originates the formation of the fractal clusters. Assuming the sticky hard-sphere potential, they calculated the phase diagram of the system and it explained the experimental observation well. On the other hand, Bouaskarne *et al.* calculated the phase diagram assuming a hard-sphere with attractive Yukawa tail between droplets [21]. Their calculated phase diagrams explain the experimental observation well, too. These results show that different models with different interaction can explain the phase behavior, that is, the interpretation of the origin of the interaction between droplets does not reach the consensus on the phase behavior. In order to shed light on this problem, the analysis of a model free structure factor is probably the best way to clarify the nature of the interaction between droplets.

In this paper, we describe the result of a SANS experiment. By applying the relative form factor method, the ϕ dependence of the intra- and inter-structures are extracted in the range of $0.05 \leq \phi \leq 0.75$ without assuming the profile of the structure factor. The ϕ dependence of the inter-droplet potential is discussed in detail.

II. RELATIVE FORM FACTOR METHOD

A coherent small-angle scattering intensity is written as follows:

$$I(q) = \langle n|f(q)|^2 s(q)\rangle, \tag{1}$$

where n is the number density of scattering objects, $|f(q)|^2$ and $s(q)$ are the form factor and the structure factor, respectively, and $\langle \cdots \rangle$ denotes the ensemble average of the thermal fluctuations of the scatterer. When the thermal fluctuations due to the form factor and the structure factor are independent of each other, Eq. (1) can be written as follows:

$$I(q) = n|\langle f(q)\rangle|^2 \langle s(q)\rangle + n[\langle |f(q)|^2\rangle - |\langle f(q)\rangle|^2]. \tag{2}$$

Neglecting the fluctuations due to the form factor, the above equation can be simply written as

$$I(q) = nF(q)S(q), \tag{3}$$

where $F(q) = |\langle f(q)\rangle|^2$ and $S(q) = \langle s(q)\rangle$. In principle, this form is applicable in the monodisperse case.

Considering the SANS contrast variation technique, $f(q)$ depends on the contrast between a scatterer and a background, $\Delta\rho$, because it is the Fourier transform of the scattering amplitude density difference between them, as follows:

$$f(q) = \int \Delta\rho(r)\exp(-iqr)dr. \tag{4}$$

On the other hand, $S(q)$ does not depend on the contrast because it indicates the time-averaged correlation of the center of mass of objects, and the properties of molecules and their assemblies do not depend on the contrast.

By using the SANS technique, it is easy to obtain different scattering contrast conditions by selective deuteration of the ingredients. A mixture of D_2O with hydrogenated oil and surfactant is called bulk contrast. In this case, only the water core is visible when the water-in-oil droplet microemulsion is formed. On the other hand, a mixture of deuterated water and oil with the hydrogenated surfactant is called film contrast. In this case, only the surfactant layer is visible to neutrons. If one changes only the scattering contrast, keeping unchanged the sample composition and the external conditions, e.g., temperature, a *relative form factor*, $R(q)$, can be introduced as the ratio of the scattering intensities from the bulk contrast, $I^b(q)$, and the film contrast, $I^f(q)$, as follows [4–6]:

$$R(q) = \frac{I^b(q)}{I^f(q)} = \frac{F^b(q)}{F^f(q)}, \tag{5}$$

i.e., the ratio of the scattering intensities of each contrast is identical to the ratio of the form factors of each contrast. This relation is independent of $S(q)$ and, therefore, one can evaluate $F(q)$ of the system without the influence of $S(q)$. We call this procedure the "relative form factor method."

In reality, the systems measured by SANS are not always the monodisperse systems, while the system has the size distribution, the membrane thickness distribution, or the directional inhomogeneity, i.e., polydispersity. In the case of polydisperse systems, Eq. (2) can be written in the following form, as described in Ref. [22]:

$$I(q) = nF(q)S_{\text{eff}}(q), \tag{6}$$

where the effective structure factor $S_{\text{eff}}(q)$ is

$$S_{\text{eff}}(q) = 1 + \beta(q)[S(q) - 1] \tag{7}$$

and $\beta(q)$ is expressed as

$$\beta(q) = \frac{|\langle f(q)\rangle|^2}{F(q)}. \tag{8}$$

$F(q)$ and $|\langle f(q)\rangle|^2$ are defined as

$$F(q) = \langle |f(q)|^2 \rangle = \int |f(q,r)|^2 h(r) dr, \tag{9}$$

$$|\langle f(q) \rangle|^2 = \left| \int f(q,r) h(r) dr \right|^2, \tag{10}$$

where r is the radius of the droplets, $h(r)$ the distribution function of r, and $f(q,r)$ the form factor of the droplets with radius r. From these relations, $\beta(q)$ and thus $S_{\text{eff}}(q)$ do depend on the scattering contrast. Note that this treatment takes the size polydispersity of droplets into account. In order to take the membrane thickness distribution into account, some other data analysis procedure, such as the procedure proposed by Gradzielski *et al.* [23,24], would be necessary.

In the case of low polydispersity, the second term in Eq. (2) can be negligibly small, and thus $\beta(q)$ and $S_{\text{eff}}(q)$ are considered to be independent of the scattering contrast. In this case, Eq. (5) can be written as follows:

$$R(q) = \frac{I^b(q)}{I^f(q)} \simeq \frac{F^b(q)}{F^f(q)}. \tag{11}$$

Therefore, the relative form factor method is valid in the small polydispersity cases.

In the present microemulsion system, we assume that the degree of the polydispersity is small enough. The formulation of $F(q)$ of droplet microemulsions has been well established by many researchers [3,9,22–24]. In the present paper, the simplest model form factor is utilized to show the validity of the relative form factor method. In the case of the bulk contrast, the form factor of a droplet with radius r_0 is

$$f^b(q,r_0) = \frac{4\pi}{3} r_0^3 (\rho_w - \rho_o) j_1(qr_0), \tag{12}$$

where ρ_w and ρ_o are the scattering length densities of water and oil, respectively, and the function $j_1(x)$ is

$$j_1(x) = 3\frac{\sin x - x\cos x}{x^3}. \tag{13}$$

On the other hand, in the case of the film contrast sample, the form factor of a droplet with the inner and the outer radius, r_0 and r_s, is as follows:

$$f^f(q,r_0) = \frac{4\pi}{3}(\rho_w - \rho_s)[r_0^3 j_1(qr_0) - A r_s^3 j_1(qr_s)], \tag{14}$$

where ρ_s is the scattering length density of the surfactant and A is defined as

$$A = \frac{\rho_o - \rho_s}{\rho_w - \rho_s}. \tag{15}$$

The outer radius of the droplets is written using the membrane thickness δ as

$$r_s = r_0 + \delta. \tag{16}$$

Using these equations, $F(q)$s for the bulk- and the film-contrast samples are obtained by the fitting of $R(q)$. Once $F(q)$ is characterized, $S_{\text{eff}}(q)$ $[S(q)]$ is obtained from the relation of Eq. (6) [Eq. (3)] in the case of the polydisperse [monodisperse] droplet system. The advantage of the method is that the assumption of the structure factor is not necessary, and that the relatively model free structure factor is obtained by only two SANS measurements with different contrast conditions.

III. EXPERIMENT

AOT (purity 99%) was purchased from Fluka [25], D_2O (99.9% atom fraction D) and deuterated n-decane (99% atom fraction D) from Isotec Inc. [25], and n-decane (purity 99%) from Katayama Chemical Co. [25]. These materials were mixed in weight without any further purification. The molar ratio of D_2O and AOT, W, was kept to 38.2 and the droplet concentration ϕ was varied from 0.05 to 0.75 with a step of 0.05. Two different contrast samples were prepared: One is the bulk contrast ($AOT/D_2O/C_{10}H_{22}$) and the other is the film contrast ($AOT/D_2O/C_{10}D_{22}$). The used values of the scattering length densities of D_2O, AOT, $C_{10}H_{22}$, and $C_{10}D_{22}$ are $\rho_{D_2O}=6.36\times10^{10}$ cm^{-2}, $\rho_{AOT}=6.42\times10^{9}$ cm^{-2}, $\rho_{C_{10}H_{22}}=-4.88\times10^{9}$ cm^{-2}, and $\rho_{C_{10}D_{22}}=6.59\times10^{10}$ cm^{-2}, respectively.

The SANS experiment was conducted on the SANS-U instrument owned by the University of Tokyo and installed at the cold neutron guide of JRR-3M in Japan Atomic Energy Research Institute (JAERI), Tokai, Japan [26–28]. 7.0 Å incident cold neutrons with a wavelength resolution of about 10% were used and the two-dimensional position sensitive proportional counter was placed at 2 m and 8 m from the sample position. The covered momentum transfer, q, ranged from (0.005 to 0.14) Å^{-1}. The sample thickness was selected to be (1 to 3) mm for optimizing the neutron transmission of the samples. The temperature was kept at $T=(298.15\pm0.2)$ K. All the obtained SANS patterns were azimuthally averaged and normalized to be the absolute unit with a Lupolen standard (a polyethylene slab calibrated with the incoherent scattering intensity of vanadium).

IV. RESULTS

The observed SANS profiles from the bulk contrast, $I^b(q)$, and the film contrast, $I^f(q)$, are shown in Figs. 1(a) and 1(b), respectively. From the bulk contrast samples, a gradual decrease of the scattering intensity with q is obtained in the low-ϕ regime, and with increasing ϕ a scattering peak due to the correlation between the water droplets appears at $q\approx0.04$ Å^{-1} for $\phi=0.3$ and shifts toward higher q [see Fig. 1(a)]. From the film contrast samples, the scattering intensity decreases with q and shows a dip at around $q\approx0.05$ Å^{-1}. The peak position at around $q\approx0.07$ Å^{-1} does not change, while the peak intensity gradually increases with increasing ϕ. In this case, the correlation peak due to the inter-droplet structure is not so remarkable in the SANS profile [see Fig. 1(b)].

The incoherent scattering intensity from the ingredients is known to be an obstruction for the analysis of the coherent SANS data [29]. Moreover, the relative form factor will have a distortion if the incoherent scattering intensity cannot be

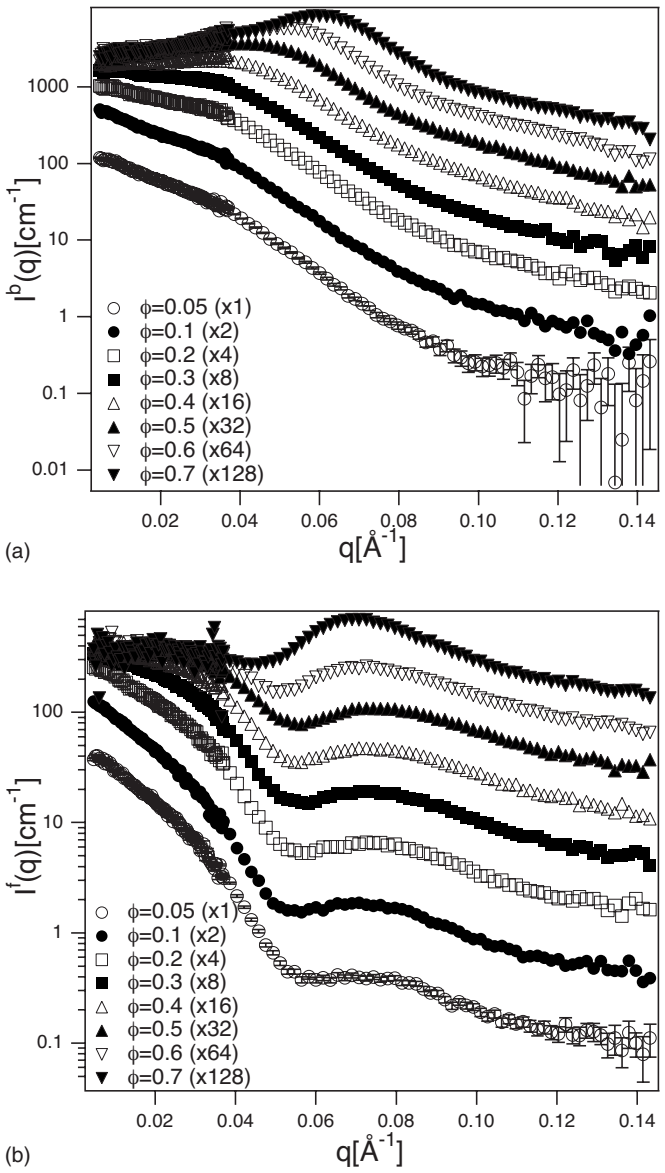

FIG. 1. ϕ dependence of the SANS profiles from (a) the bulk contrast and (b) the film contrast. The scattering intensity from $\phi=0.05$ is shown in absolute units, and the others are shifted as shown in the legend for better visualization. The error bars shown in this text indicate ±1 standard deviation.

negligibly small. In the low-q region, for both the contrast cases, it is expected that the coherent scattering intensity, I_{coh}, is much higher than the incoherent scattering intensity, I_{inc}. When I_{coh} is two orders of magnitude larger than I_{inc}, the distortion of $R(q)$ due to the incoherent background is expected to be less than 1% after the subtraction of I_{inc}. On the other hand, in the low concentration and at high q, there are possibilities of $I_{coh} \approx I_{inc}$. In this case, even after the subtraction of I_{inc} from the observed scattering intensities, $R(q)$ may have a considerable distortion due to the incoherent background. For example, if I_{inc} is estimated within the accuracy of 90%, the distortion of $R(q)$ is expected to be about 10%. The important message here is that it is necessary to subtract the contribution of I_{inc} from the scattering intensity as precisely as possible, if the contribution of I_{inc} is expected to be above 10% of the scattering intensity.

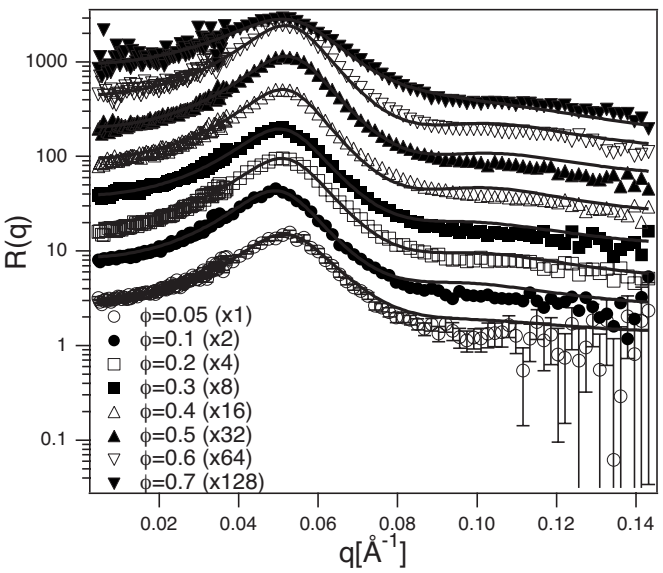

FIG. 2. ϕ dependence of $R(q)$s. $R(q)$ for $\phi=0.05$ is shown as it is and the others are shifted as shown in the legend for better visualization.

In our experiment and data analysis, the sample thickness dependence of the SANS intensity from D_2O, protonated and deuterated decane were measured to estimate the incoherent scattering intensity of the mixtures. The estimated values of the incoherent scattering intensities, which are obtained taking the contributions from the sample thickness and the composition into account, are subtracted from the scattering intensities of the microemulsions. In our case, the maximum distortion of $R(q)$ by the incoherent scattering intensity is calculated to be about 5% at $q \approx 0.08$ Å^{-1} for $\phi=0.05$. This value of the distortion is the largest influence in the present result and we neglect the distortion of $R(q)$ due to the incoherent scattering intensity in this paper.

A. Form factor

The obtained $R(q)$s for various ϕ in the whole-q range are shown in Fig. 2. It is clear that $R(q)$s below $\phi \approx 0.6$ have almost the same profile. Since $R(q)$ is sensitive to the change of the form factor, this result indicates that the droplet shape is unchanged below $\phi \approx 0.6$. The profile change of $R(q)$ at $\phi > 0.6$ indicates the deformation of the droplet structure of the unit particle.

In the present analysis the Gaussian distribution function,

$$h(r) = \frac{1}{\sqrt{2\pi}\Delta r} \exp\left[-\left(\frac{r - r_0}{\sqrt{2}\Delta r} \right)^2 \right], \tag{17}$$

is used as the size distribution function in Eq. (9) for simplicity instead of the Schultz size distribution function, which has been generally used in AOT microemulsion systems [22]. r_0 is the mean radius of the water droplets and Δr the root mean square deviation from the mean of droplets as

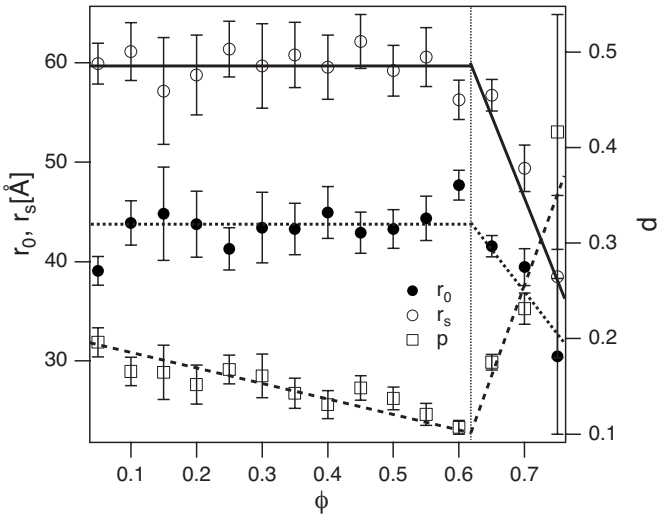

FIG. 3. ϕ dependence of the structural parameters of the droplet shape. r_0 and r_s are indicated with the left vertical axis unit, and p with the right vertical axis unit. The vertical dotted line indicates the concentration of ϕ^*. The solid, dotted, and dashed lines are guides for the eyes.

$$\Delta r^2 = \langle r_0^2 \rangle - \langle r_0 \rangle^2. \tag{18}$$

The calculation was performed in the case only for $r>0$. The polydispersity index p_{exp} is expressed as $p_{\mathrm{exp}}=\Delta r/r_0$. It is known that the differences between the Gaussian and the Schultz size distribution functions are small in low polydispersity cases.

The solid lines in Fig. 2 are fit results according to Eq. (11). Fit parameters are r_0, Δr, and the membrane thickness of droplets, δ. The polydispersity index, p, is calculated as $p^2=p_{\mathrm{exp}}^2-p_{\mathrm{res}}^2$, where p_{exp} is obtained from the fit parameters. Basically the instrumental resolution affects the value of p, and this part, p_{res}, is subtracted from p_{exp}, as mentioned above. The value of $p_{\mathrm{res}}=0.13$ is assumed according to the measurement of the q resolution of the SANS-U spectrometer [30]. The fit result shown in Fig. 2 explains the experimental spectra well at least in the range of $q \leq 0.08$ Å^{-1}.

The ϕ dependence of the obtained fit parameters are shown in Fig. 3. The mean radius of the droplet shell, r_s, is calculated from $r_s=r_0+\delta$. r_0 and r_s are almost constant below $\phi^* \approx 0.62$, and they decrease above ϕ^*. The mean values of r_0 and r_s at $\phi \leq 0.6$ are (43.6±0.6) Å and (59.7±0.5) Å, respectively. The value of p decreases monotonically below ϕ^*, and then it increases with ϕ. The slope at $\phi \leq 0.6$ is $dp/d\phi \approx -0.12$ and it is close to the result obtained by Kotlarchyk *et al.* [9] at $W=40.8$, $0.04 \leq \phi \leq 0.21$, and $T \approx 295$ K. These results indicate that the size of the water droplets does not change, while the polydispersity decreases with increasing ϕ below $\phi=\phi^*$. The size distribution of droplets becomes minimum at $\phi=\phi^*$, and at $\phi>\phi^*$ it tends to increase. The value of ϕ^* is close to the value of the glasslike transition concentration $\phi_c \approx 0.65$ obtained by Sheu *et al.* [19], where the macroscopic viscosity tends to diverge. The concentration dependence of the macroscopic viscosity is explained by the structure change of the droplets described here.

Above $\phi=0.65$, the value of p increased drastically. In this ϕ region, the Gaussian distribution function may not be appropriate to explain the experimental result, since this function is valid only for the small polydispersity case. In order to check the validity of the Gaussian distribution function in this ϕ region, we analyzed the data using the log-normal distribution function instead of the Gaussian function. In our calculation, the ϕ dependence of the structure parameters showed almost the same tendency for both distribution functions. Thus the data points shown at $\phi \geq 0.65$ have few meanings, while those points remind us of the idea of the deformation of the sphere in the high concentration region.

As explained in Sec. II, the size polydispersity affects the profile of $R(q)$, and thus the estimated structure parameters may be changed when we consider the effect of $\beta(q)$. In order to estimate the effect of $\beta(q)$ on the structure parameters of the form factor, we reanalyzed $R(q)$ taking $\beta(q)$ into account. According to our calculation, the effect of $\beta(q)$ appears at low-q region as a distortion of $R(q)$. Due to the distortion of $R(q)$, p decreased about 10%, while r_0 and δ remained almost the same values. This result indicated the profile of the form factor is almost the same even when the effect of polydispersity is taken into account.

In the present paper, only a slight deviation is obtained between the experimental observation and the fit result without the consideration of $\beta(q)$. The origin of the deviation comes from the limitation of the model form factor, such as distribution of the membrane thickness, as well as the effect of $\beta(q)$. Our result shows that the relative form factor can be applied when the polydispersity is less than $p=0.15$. However, it should be noted that the larger value of p originates the large discrepancy between $S(q)$ and $S_{\mathrm{eff}}(q)$ according to the relation of Eq. (7).

The form factors, $F^b(q)$ and $F^f(q)$, are reproduced from the estimated structure parameters without taking the effect of $\beta(q)$ into account. In order to compare the results of the reproduced form factors with the observed SANS profiles, the number density n was multiplied to $F^b(q)$ and $F^f(q)$. The value of n was estimated from both the experimental result, so as to get $S(q) \approx 1$ in the high-q region, and the calculation. For example, the value of n for $\phi=0.05$ of the bulk contrast sample is estimated to be $n \approx 4 \times 10^{16}$ cm^{-3}. This value is consistent with the calculated value of the number density, $n_{\mathrm{calc}}=\phi/(4\pi r_0^3/3) \approx 5 \times 10^{16}$ cm^{-3} for $\phi=0.05$.

In Fig. 4, the reproduced $F^b(q)$ and $F^f(q)$ are shown for $\phi=0.05$ with the observed SANS profile. This figure clearly indicates that the obtained SANS profile and the reproduced form factor are different in the low-q region. The origin of the deviation is ascribed to the contribution from the structure factor. This fact implies that the structure factor of the droplet microemulsion systems cannot be unity even when the concentration of the water droplets is low at room temperature.

B. Structure factor

Following the successful estimation of $F(q)$s, we calculated the concentration dependence of $S_{\mathrm{eff}}(q)$ as a ratio of

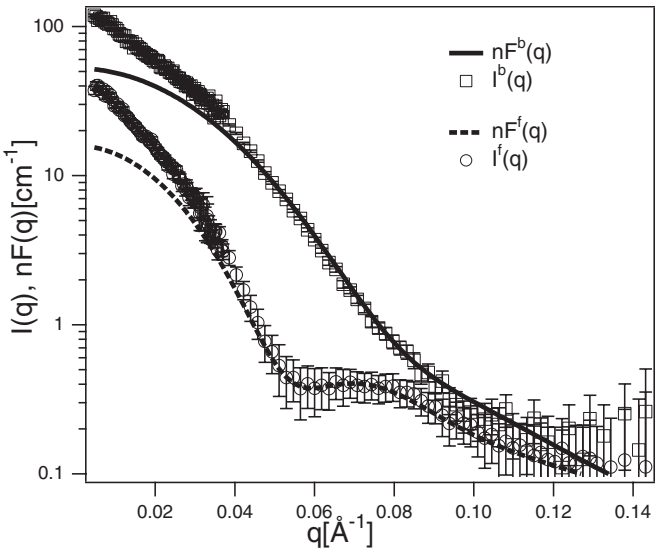

FIG. 4. Reproduced $F^b(q)$ and $F^f(q)$ as well as the experimentally observed SANS profiles, $I^b(q)$ and $I^f(q)$, for $\phi=0.05$. $F^b(q)$ and $F^f(q)$ are multiplied by the number density, n, in order to compare with SANS profiles.

$I(q)$ and $nF(q)$ according to Eq. (6). In Fig. 5, the concentration dependence of $S_{\text{eff}}(q)$ with ϕ between 0.05 and 0.75 is shown below $q=0.08$ Å^{-1} for the bulk contrast sample. The evaluated $S^b_{\text{eff}}(q)$ is almost the same as $S^f_{\text{eff}}(q)$ in this q range. This result is one of the most important results in the present paper, that is, the structure factor is evaluated without any assumptions on the spatial distribution of droplets or the interaction between droplets except for the assumption of the shape of the droplets.

In general, the structure factor is determined by the disposition of the unit particles or the inter-particle interaction. This means that determining the model free structure factor is essential for the understanding the physical properties of the system. From this point of view, we explain what kind of

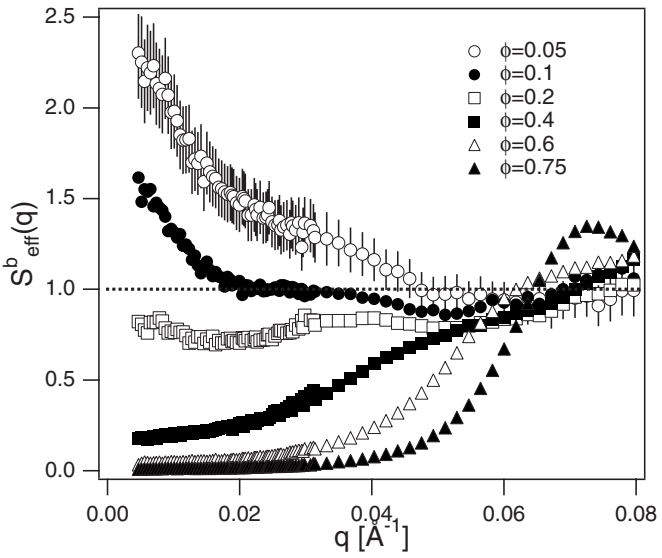

FIG. 5. ϕ dependence of the evaluated $S^b_{\text{eff}}(q)$. The error bars are shown only for $\phi=0.05$.

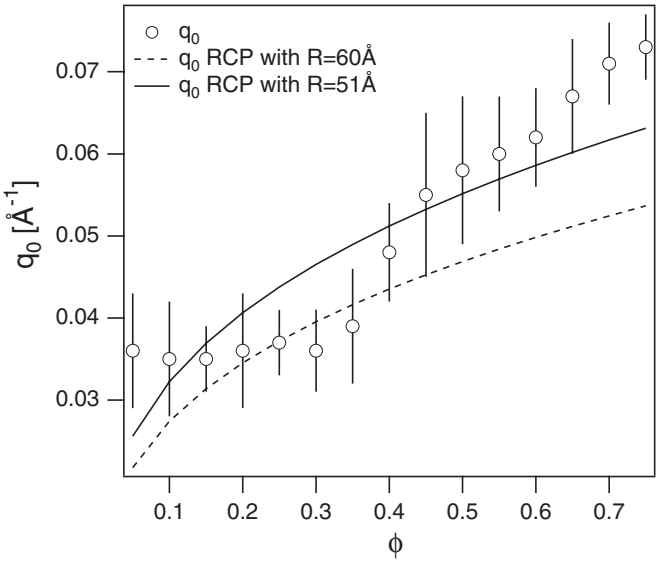

FIG. 6. ϕ dependence of the peak position q_0 evaluated from $S^b_{\text{eff}}(q)$. The solid and dashed lines indicate the calculated peak position assuming the random closed packing of a sphere with its radius of 51 and 60 Å, respectively.

information is obtained from the estimated $S_{\text{eff}}(q)$s, since no model structure factor, unfortunately, can explain the profile of the present result.

In the low-ϕ region ($\phi \lesssim 0.25$), $S_{\text{eff}}(q)$ tends to increase with decreasing q below $q \approx 0.03$ Å^{-1}. This behavior is observed when the concentration fluctuations are essential for the structure formation. In the case of the AOT microemulsion system, a phase separation from one-phase droplets to two-phase droplets associated with a critical phenomenon has been discussed with increasing temperature [9–14]. The origin of the phase separation at high temperature is the increase of the interdroplet attractive interaction with temperature. The increase of $S_{\text{eff}}(q)$ in the low-q region with decreasing q is due to the large concentration fluctuations.

In the medium-q range from (0.02 to 0.04) Å^{-1}, a broad peak is observed at $q \approx 0.03$ Å^{-1}. As shown in Fig. 6, the peak position, q_0, seems to be independent of the concentration of the droplets at $\phi < 0.4$, although the error is very large. The peak intensity seems to change with increasing ϕ. This tendency of the peak is similar to the characteristic feature of the so-called "cluster peak," recently observed in the lysozyme aqueous solution [31–35]. According to the discussion in the literature, the characteristic features of the cluster peak are that the peak position is independent of the concentration of the sample, while the peak intensity depends on the concentration. The cluster peak appears when the short-range attraction and the long-range repulsion are competing in the system. In the AOT microemulsion system, the cluster formation of the system has been established experimentally before [16]. Although the physical properties of the cluster peak are not completely clarified yet, the present result suggests the existence of the long-range repulsion in this system. So far, the hard-sphere repulsion and the short-range attraction have been employed to explain the phase behavior and the scattering profiles in the AOT microemulsion systems.

However, in some cases, the assumption of the long-range attraction was necessary to explain the experimental result [14]. These complexities of the interaction among droplets could be the essential features of the colloidal systems and be one of future problems.

In the higher-ϕ region above $\phi=0.3$, $S_{\mathrm{eff}}(q)$ shows the characteristic feature of the hard-sphere model structure factor, which has a small osmotic compressibility and a peak at finite q with oscillation of $S_{\mathrm{eff}}(q)$ around unity. In this case, the peak position shifts toward higher q with ϕ. Figure 6 shows a clear peak shift with increasing ϕ above $\phi\approx 0.4$. The lines in the figure show the peak position if the random closed packing is assumed for the sphere with its radius of 60 Å (dashed line) and 51 Å (solid line), respectively. The shell radius of the droplet was estimated to be about 60 Å in the present microemulsion. However, the estimated peak position seems to follow the case of 51 Å at $0.4\leq\phi\leq 0.6$. This length scale is corresponding to the core size plus half the membrane thickness. This coincidence occurs due to the overlapping of the surfactant tails of the neighboring droplets. At $\phi\geq 0.65$, the estimated peak position is larger than the calculated one with the radius of 51 Å. This fact implies again that the droplet shape is changed at $\phi\geq 0.65$.

So far, Bagger-Jörgensen *et al.* showed a broad profile of the structure factor in a microemulsion system composed of pentaethylene glycol dodecyl ether ($C_{12}E_5$), decane, and D_2O [36]. They claimed that the experimentally obtained $S(q)$ in the whole-q range at small-angle region is not so simply explained by the model structure factor of the hard-sphere potential, although the concentration dependence of $S(q=0)$ is relatively simple [36]. The present result indicates that any model structure factor cannot explain the structure factor of the microemulsion system in the whole-q range as well. The origin of the broadness of the structure factor is ascribed to the fact that the system has size polydispersity and also that the unit particle is a soft-sphere droplet. The modification of the model structure factor for the soft-sphere case rather than the hard-sphere will help to understand the profile of the present structure factor.

V. DISCUSSION

In this section, we discuss the ϕ dependence of $S(q=0)$, since the characteristic feature of the ϕ dependence of the inter-droplet interaction can be described in the long wavelength limit of the structure factor. The inter-particle potential is estimated from two different types of models. One is an aggregation model proposed by Koper *et al.* [15], since the obtained structure factor showed a cluster peak-like behavior as explained above. The other is the square well potential model proposed by Baxter [16,37], which has been used as a model structure factor for the AOT microemulsion system. The ϕ dependence of $S_{\mathrm{eff}}(0)$ is shown in Fig. 7. The value of $S_{\mathrm{eff}}(0)$ is obtained by the extrapolation of $S_{\mathrm{eff}}(q)$ toward $q=0$ according to a Lorentzian function.

Koper *et al.* [15] proposed an osmotic equation of state within the consideration of the inter-droplet attractive interaction for a similar microemulsion system, composed of AOT, water, and iso-octane. They assumed that the droplets

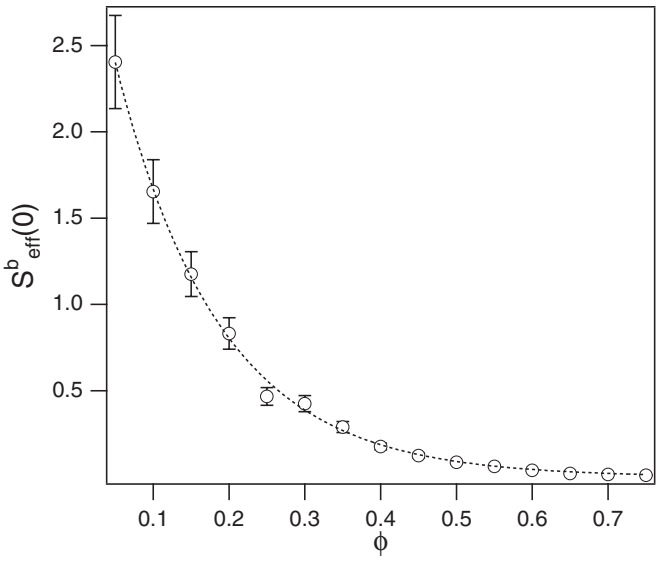

FIG. 7. ϕ dependence of $S^b_{\mathrm{eff}}(0)$ of the bulk contrast samples. The dashed line is a guide for the eyes.

aggregate linearly so that the droplet clusters are formed. The interaction between the droplets is assumed to be short ranged. A linear k-cluster is formed by k droplets and has $k-1$ bonds. The binding free energy per bond, B, is assumed to be constant. Then they expressed the osmotic pressure, Π, of the droplets as follows [15]:

$$\frac{\Pi v_d}{k_B T} = \phi + \left[4 - \exp\left(-\frac{B}{k_B T}\right)\right]\phi^2 + \cdots, \tag{19}$$

within the calculation of the virial expansion for the osmotic pressure, where v_d, k_B, and T indicate the volume of the droplets, the Boltzmann constant, and temperature, respectively.

$S(0)$ evaluated from the structure factor is inversely proportional to the osmotic compressibility, $d\Pi/d\phi$, as [38]

$$S(0) = \frac{k_B T}{v_d}\left(\frac{\partial \Pi}{\partial \phi}\right)^{-1}. \tag{20}$$

Combining Eqs. (19) and (20), a relationship between B and $S(0)$ is derived as follows:

$$-\frac{B}{k_B T} = \ln\left[4 - \frac{S(0)^{-1} - 1}{2\phi}\right]. \tag{21}$$

Here, we used the value of $S_{\mathrm{eff}}(0)$ as $S(0)$ in Eq. (21). Figure 8 shows the ϕ dependence of the binding free energy per bond, B (full square). B increases with ϕ, and this means that the attractive interaction between droplets becomes weak with increasing ϕ. In the higher concentration region above $\phi=0.3$, the model is not valid due to the many body problems. The extracted value of B is in the order of $k_B T$, and, unfortunately, does not validate the virial expansion like Eq. (19). Thus we conclude that the cluster formation mechanism in this system is not as simple as that modeled by Koper *et al.* [15].

Another model to compare with the present experimental result is that of the square well potential, originally proposed

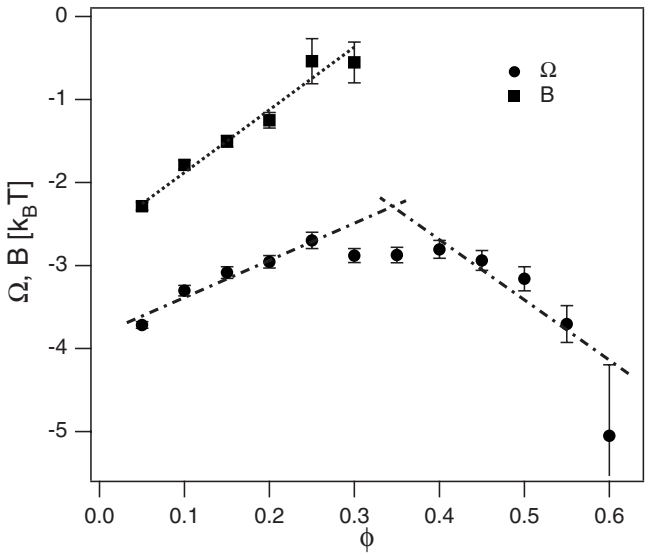

FIG. 8. Concentration dependence of the binding free energy, B, and the depth of the inter-droplet potential, Ω. The vertical axis is shown in units of k_BT. Below $\phi \approx 0.4$, both the values of B and Ω tend to increase with ϕ; on the other hand, above $\phi \approx 0.4$ Ω tends to decrease. The lines are guides for the eyes.

by Baxter [37] and modified by Liu *et al.* [39]. This model has been successfully used as a model structure factor for SAXS or SANS data analyses [39–42].

In this model the pairwise inter-particle interaction potential, $V_B(r)$, is assumed as

$$\frac{V_B(r)}{k_BT} = \begin{cases} +\infty & \text{for } 0 < r < R', \\ \Omega & \text{for } R' < r < R, \\ 0 & \text{for } R < 0, \end{cases} \tag{22}$$

where R indicates the droplet diameter and the attractive potential with the potential depth of Ω is existing at the droplet surface and its osmotic depth is expressed by $R-R'$. The dimensionless parameter, τ, which is called the stickiness parameter, expresses the strength of the stickiness, and is related to Ω as follows:

$$\Omega = \ln[12\epsilon\tau], \tag{23}$$

where the fractional surface layer thickness, ϵ, is $\epsilon=(R-R')/R$.

The expression of $S(q)$ was derived within the treatment of the Percus-Yevick approximation [43], and is given, for example, in Eq. (5) of Ref. [44]. The solution for $q=0$ is expressed as a function of λ:

$$S(0)^{-1} = X\lambda^2 + Y\lambda + Z. \tag{24}$$

The physical meaning of the parameter λ is not clear but may be thought of as an attractive energy scale [44]. The other parameters in Eq. (24) are functions of η and ϵ as

$$X = \frac{\eta^2}{(1-\eta)^2} - \frac{\eta^2}{6}\epsilon^2, \tag{25}$$

$$Y = \epsilon\eta - \frac{2\eta(2\eta+1)}{(1-\eta)^3}, \tag{26}$$

$$Z = \frac{(1+2\eta)^2}{(1-\eta)^4} - 8\eta(\epsilon^3 - 3\epsilon^2 + 3\epsilon), \tag{27}$$

where η is the effective volume fraction and it is related to ϕ as

$$\eta = \frac{\phi}{(1-\epsilon)^3} \approx \frac{\phi}{1-3\epsilon}. \tag{28}$$

The concentration dependence of λ is expressed using $S(0)$ as

$$\lambda = \frac{-Y \pm \sqrt{Y^2 - 4X[Z - S(0)^{-1}]}}{2X}. \tag{29}$$

From Eq. (8) in Ref. [44], τ is a function of η, λ, and ϵ as follows:

$$\tau = \frac{\eta\lambda}{12}\left(1 + \frac{3\epsilon\eta}{1-\eta}\right) + \frac{1}{2\lambda(1-\eta)^2}[2 + \eta - 12\epsilon\eta(1-\eta)] - \frac{\eta}{1-\eta}\left(1 - \frac{1 - 11\eta/4 + \eta^2}{1-\eta}\epsilon\right). \tag{30}$$

The concentration dependence of τ is estimated from $S(0)$ assuming the value of $\epsilon=0.02$ from the combination of Eqs. (28)–(30). This value of ϵ is of the same order of magnitude as the one reported in literature [16,39]. The value of $S_{\text{eff}}(0)$ is used as $S(0)$ in Eq. (29).

Using Eq. (23), Ω was calculated as shown in Fig. 8 (full circles). As seen from the figure, the value of Ω tends to increase in the low-ϕ regime up to $\phi \approx 0.3$. This means that the stickiness decreases with increasing ϕ below $\phi \approx 0.3$. This result is consistent with the ϕ dependence of B shown above. The ϕ dependence of the value of τ has been described by Chen *et al.* [16] and by Robertus *et al.* [40] in the low-ϕ region, and their results are consistent with the present results.

On the other hand, Ω decreases with increasing ϕ above $\phi \approx 0.4$. In the high-ϕ region, Seto *et al.* estimated the ϕ dependence of Ω by SAXS, and they concluded that the inter-droplet attraction increased with increasing ϕ [20]. This result is consistent with the present result. The increase of the attractive interaction with ϕ may originate from the increase of the overlapping of the tails of surfactant in the high-ϕ region. As a matter of fact, from the result of the ϕ dependence of the peak position shown in Fig. 6, the overlapping of the surfactant tails of the neighboring droplets is suggested.

It is noteworthy that the value of ϕ is about 0.4 where the phase behavior in the phase diagram changes. In the lower-ϕ region, a phase separation from the one-phase droplet to the two-phase droplet occurs, while in the higher-ϕ region, a phase transition from the one-phase droplet to a lamellar phase occurs with increasing temperature. (See Fig. 1 in Ref. [17].) The present result suggests that the change of the characteristic feature of the droplet-droplet interaction leads to a different structural formation and to the phase transitions.

A clear ϕ dependence of the interaction parameter between droplets is extracted from both models applied in the present paper. However, there is no reason to change the strength of the attraction between the droplets with changing the density of the droplets within the consideration of the pair potential. This means that the inter-droplet interaction is not expressed by the simple pair potential even in the long wavelength limit. In reality, more complex interaction models, which are considering the many body problems, soft-sphere interaction potential, and so on, would be necessary to explain the present structure factor.

Here, we summarize the considerable problems for understanding the actual structure factor: The size polydispersity of the system affects the profile of the effective structure factor even in the long wavelength limit; the droplets do not have the simple pair potential of the hard-sphere interaction; the many body potential is effective even in the present concentration region, especially, if the interaction potential has a directional inhomogeneity, then the potential depth would depend on the concentration of the unit particles.

As demonstrated by the data displayed in Fig. 5, the droplets are strongly interacting in the whole range of investigated volume fractions. This might be accounted for by the modified Baxter model (nonperturbative, though approximate), if it were suitable to disregard the strange dependence of Ω on ϕ—an artifact of the Percus-Yevick treatment of a too simple model, Eq. (22), presumably.

The present result indicates a complicated picture for the interaction between droplets depending on the concentration, although the phase behavior has been well explained by some simple models in the AOT microemulsion systems so far. This complexity of the interaction between droplets might be the reason why different phase transitions are observed in the low-ϕ region and in the high-ϕ region.

VI. CONCLUSIONS

We discussed the droplet density dependence of the static structure factor in a ternary microemulsion consisting of AOT, water, and decane. By introducing the relative form factor method, we obtained a droplet density dependence of the form factor without any assumptions of the profile of the structure factor. The evaluated droplet radius was almost constant, while the polydispersity decreased with increasing ϕ below $\phi \approx 0.6$. The shape change of the water droplets was confirmed at $\phi > 0.6$.

We also evaluated a droplet density dependence of the structure factor for the whole droplet density range measured. At low concentration, $\phi \leq 0.25$, an upturn of the structure factor in the low-q region was obtained, while above $\phi = 0.25$ such an upturn was not observed. A peak, whose characteristic features are similar to the cluster peak [31–35], is obtained in the system. The structure factor cannot be explained by any model structure factors at present. This fact indicates that the interaction between droplets is not so simple even in the AOT microemulsion system.

The advantage of the relative form factor method is that the form factor and the structure factor can be extracted without any assumptions on the structure factor even in the dense droplet region.

ACKNOWLEDGMENTS

We thank Professor Mitsuhiro Shibayama at the University of Tokyo for his discussion. We also appreciate Dr. Paul Butler and Dr. Antonio Faraone at the National Institute of Standards and Technology for their critical readings and discussion about this paper. We would like to express our gratitude to the referees of this paper for their valuable comments to upgrade the paper. One of the authors (M.N.) was supported by the Grant-in-Aid for Encouragement of Young Scientists (B) (No. 13740234 and 15740260) from the Japanese Ministry of Education, Culture, Sports, Science and Technology, when M.N. was a member of the University of Tokyo. The SANS experiment was done under approval of the Neutron Scattering Program Advisory Committee (Proposal No. 01-202).

[1] O. Glatter, J. Appl. Crystallogr. **14**, 101 (1981).
[2] G. Fritz, A. Bergmann, and O. Glatter, J. Chem. Phys. **113**, 9733 (2000).
[3] L. Arleth and J. S. Pedersen, Phys. Rev. E **63**, 061406 (2001).
[4] A. L. Rollet, O. Diat, and G. Gebel, J. Phys. Chem. B **106**, 3033 (2002).
[5] M. Nagao, H. Seto, M. Shibayama, and N. L. Yamada, J. Appl. Crystallogr. **36**, 602 (2003).
[6] M. Nagao, H. Seto, M. Shibayama, and T. Takeda, Physica B **385-386**, 783 (2006).
[7] L. Rubatat, G. Gebel, and O. Diat, Macromolecules **37**, 7772 (2004).
[8] L. Rubatat, Z. Shi, O. Diat, S. Holdcroft, and B. J. Frisken, Macromolecules **39**, 720 (2006).
[9] M. Kotlarchyk, S. H. Chen, J. S. Huang, and M. W. Kim, Phys. Rev. A **29**, 2054 (1984).
[10] M. Kotlarchyk, S. H. Chen, J. S. Huang, and M. W. Kim, Phys. Rev. Lett. **53**, 941 (1984).
[11] S. H. Chen, S. L. Chang, and R. Strey, J. Chem. Phys. **93**, 1907 (1990).
[12] H. Seto, D. Schwahn, K. Mortensen, and S. Komura, J. Chem. Phys. **99**, 5512 (1993).
[13] H. Seto, D. Schwahn, E. Yokoi, M. Nagao, S. Komura, M. Imai, and K. Mortensen, Physica B **213&214**, 591 (1995).
[14] H. Seto, D. Schwahn, M. Nagao, E. Yokoi, S. Komura, M. Imai, and K. Mortensen, Phys. Rev. E **54**, 629 (1996).
[15] G. J. M. Koper, W. F. C. Sager, J. Smeets, and D. Bedeaux, J. Phys. Chem. **99**, 13291 (1995).
[16] S. H. Chen, J. Rouch, F. Sciortino, and P. Tartaglia, J. Phys.: Condens. Matter **6**, 10855 (1994).
[17] C. Cametti, P. Codastefano, P. Tartaglia, S. H. Chen, and J. Rouch, Phys. Rev. A **45**, R5358 (1992).
[18] M. Nagao, H. Seto, T. Takeda, and Y. Kawabata, J. Chem. Phys. **115**, 10036 (2001).

[19] E. Y. Sheu, S. H. Chen, J. S. Huang, and J. C. Sung, Phys. Rev. A **39**, 5867 (1989).
[20] H. Seto, M. Nagao, Y. Kawabata, and T. Takeda, J. Chem. Phys. **115**, 9496 (2001).
[21] M. Bouaskarne, S. Amokrane, and C. Regnaut, J. Chem. Phys. **111**, 2151 (1999).
[22] M. Kotlarchyk and S. H. Chen, J. Chem. Phys. **79**, 2461 (1983).
[23] M. Gradzielski, D. Langevin, T. Sottmann, and R. Strey, J. Chem. Phys. **106**, 8232 (1995).
[24] M. Gradzielski, D. Langevin, and B. Farago, Phys. Rev. E **53**, 3900 (1996).
[25] Certain commercial equipment, instruments, or materials are identified in this paper to foster understanding. Such identification does not imply recommendation or endorsement by the National Institute of Standards and Technology, nor does it imply that the materials or equipment identified are necessarily the best available for the purpose.
[26] Y. Itoh, M. Imai, and H. Takahashi, Physica B **213&214**, 889 (1995).
[27] S. Okabe, M. Nagao, T. Karino, S. Watanabe, and M. Shibayama, J. Appl. Crystallogr. **38**, 1035 (2005).
[28] S. Okabe, T. Karino, M. Nagao, S. Watanabe, and M. Shibayama, Nucl. Instrum. Methods Phys. Res. A **572**, 853 (2007).
[29] M. Shibayama, M. Nagao, S. Okabe, and T. Karino, J. Phys. Soc. Jpn. **74**, 2728 (2005).
[30] This value of p_{res} is a typical value of the q resolution for the SANS-U instrument. Although p_{res} depends on q, the smearing effects mainly appear at around the dip or the peak position. Thus, the value of p_{res} is estimated at $q \approx 0.06$ Å^{-1}.
[31] A. Stradner, H. Sedgwick, F. Cardinaux, W. C. K. Poon, S. U. Egelhaaf, and P. Schurtenberger, Nature (London) **432**, 492 (2004).
[32] F. Sciortino, S. Mossa, E. Zaccarelli, and P. Tartaglia, Phys. Rev. Lett. **93**, 055701 (2004).
[33] A. Stradner, G. M. Thurston, and P. Schurtenberger, J. Phys.: Condens. Matter **17**, S2805 (2005).
[34] Y. Liu, E. Fratini, P. Baglioni, W.-R. Chen, and S.-H. Chen, Phys. Rev. Lett. **95**, 118102 (2005).
[35] Y. Liu, W.-R. Chen, and S.-H. Chen, J. Chem. Phys. **122**, 044507 (2005).
[36] H. Bagger-Jörgensen, U. Olsson, and K. Mortensen, Langmuir **13**, 1413 (1997).
[37] R. J. Baxter, J. Chem. Phys. **49**, 2770 (1968).
[38] See, for example, H. Mays, K. Mortensen, and W. Brown, in *Scattering in Polymeric and Colloidal Systems*, edited by W. Brown and K. Mortensen (Gordon and Breach Science Publishers, Amsterdam, 2000), pp. 249–325.
[39] Y. C. Liu, S. H. Chen, and J. S. Huang, Phys. Rev. E **54**, 1698 (1996).
[40] C. Robertus, W. H. Philipse, J. G. H. Joosten, and Y. K. Levine, J. Chem. Phys. **90**, 4482 (1989).
[41] H. Seto, D. Okuhara, Y. Kawabata, T. Takeda, M. Nagao, J. Suzuki, H. Kamikubo, and Y. Amemiya, J. Chem. Phys. **112**, 10608 (2000).
[42] M. Nagao, H. Seto, and Y. Kawabata, J. Phys. Soc. Jpn. Suppl. A **70**, 335 (2001).
[43] J. K. Percus and G. J. Yevick, Phys. Rev. **110**, 1 (1958).
[44] G. Foffi, E. Zaccarelli, F. Sciortino, P. Tartaglia, and K. A. Dawson, J. Stat. Phys. **100**, 363 (2000).